Earth and Planetary Science Letters 597 (2022) 117793

Contents lists available at ScienceDirect

Earth and Planetary Science Letters

www.elsevier.com/locate/epsl

Mantle source characteristics and magmatic processes during the 2021 La Palma eruption

James M.D. Day [a,*], Valentin R. Troll [b,c,d], Meritxell Aulinas [e,f], Frances M. Deegan [b,c], Harri Geiger [g], Juan Carlos Carracedo [d], Guillem Gisbert Pinto [e], Francisco J. Perez-Torrado [d]

[a] Scripps Institution of Oceanography, University of California San Diego, La Jolla, CA 92093, USA
[b] Department of Earth Sciences, Natural Resources & Sustainable Development (NRHU), Uppsala University, 75236 Uppsala, Sweden
[c] Centre for Natural Hazard and Disaster Science (CNDS), Uppsala University, 75236 Uppsala, Sweden
[d] Instituto de Estudios Ambientales y Recursos Naturales (i-UNAT), University of Las Palmas de Gran Canaria (ULPGC), 35017 Las Palmas de Gran Canaria, Spain
[e] Departament de Mineralogia, Petrologia i Geologia Aplicada, University of Barcelona, Marti Franques s/n, 08028, Barcelona, Spain
[f] Geomodels Research Institute, University of Barcelona, Marti Franques s/n, 08028, Barcelona, Spain
[g] Institute of Earth and Environmental Sciences, University of Freiburg, 79104 Freiburg im Breisgau, Germany

ARTICLE INFO

Article history:
Received 13 May 2022
Received in revised form 24 August 2022
Accepted 26 August 2022
Available online 22 September 2022
Editor: C.M. Petrone

Keywords:
La Palma
2021 eruption
lava chemistry
olivine
pyroxene
oxygen fugacity

ABSTRACT

The 2021 eruption of La Palma (September 19-December 13) was the first subaerial eruption in the Canary Islands in 50 years. Approximately 0.2 km^3 of lava erupted from a newly formed, broadly basaltic composite volcanic edifice on the northwestern flank of the Cumbre Vieja volcanic ridge. Comprehensive sampling of the olivine- and clinopyroxene-phyric lavas over the eruption period reveals temporal changes in mineralogy and bulk rock geochemistry from tephrite to basanite. Initial tephrite lavas have low MgO (~6 wt.%) and elevated TiO_2 (~4 wt.%) and contain amphibole crystals and gabbroic micro-xenoliths. In contrast, lavas with progressively more mafic compositions erupted to approximately day 20 of the eruption and thereafter remained as basanite (~8 wt.% MgO; 3.7 wt.% TiO_2) until eruption termination. Temporal changes in lava chemistry reflect initial eruption of fractionated magmas that crystallized 5-10% olivine and clinopyroxene, as well as minor spinel, sulfide, and magnetite, followed by later eruption of deeper-sourced and more primitive magma. Vanadium-in-olivine oxybarometry indicates parental magmas were oxidized (fO_2 = +1.5 to +2 FMQ) with 8.2 ±0.8 wt.% MgO and were generated from between 2.5-3% partial melting of a mantle source potentially containing a pyroxenite component (X_{px} = 0.31 ±0.12). Day 1-20 tephrites have more radiogenic $^{187}Os/^{188}Os$ (0.143-0.148) and lower Pd, Pt, Ir and Os contents than post day 20 basanites ($^{187}Os/^{188}Os$ = 0.141-0.145). Combined with available seismic data, the lavas provide a high-resolution record of eruptive evolution. Initial fractionated tephrite magma was stored in the upper lithosphere up to four years prior to eruption, consistent with precursor seismicity and the presence of partially reacted amphibole and micro-xenoliths. The later lavas of the eruption were fed by more primitive basanitic parental magmas that were likely sourced from the deeper portion of the magma storage system that is underplating the island. Precursor events to the 2021 La Palma eruption involved seismicity and magma emplacement, storage and differentiation, which was followed by mobilisation, eruption, and eventual exhaustion of stored magma and partial melts. This magmatic progression is similar to that documented from the 1949 and 1971 Cumbre Vieja eruptions. Ocean islands with limited basaltic magma supply show similarities to the magmatic evolution observed in large silicic systems, where initial magma emplacement and differentiation is followed by later magma remobilisation that induces volcanic activity.

1. Introduction

The 2021 eruption on the Cumbre Vieja ridge of La Palma was the first subaerial eruption in the Canary Islands for 50 years and one of the best monitored eruptions on any ocean island to date. The 2021 La Palma eruption therefore offers an unprecedented opportunity to examine magmatic processes, including temporal geochemical variations associated with ocean island basalt (OIB) systems. As with many OIB localities globally, the Canary Islands form an age-progressive hotspot track, with magmatism likely generated by anomalous partial melting induced from a deeply derived man-

* Corresponding author.
E-mail address: jmdday@ucsd.edu (J.M.D. Day).

https://doi.org/10.1016/j.epsl.2022.117793

tle plume (Hoernle et al., 1995; Carracedo et al., 1998; Zaczek et al., 2015). Previous studies have shown that Canary Island volcanoes in general (Hoernle and Schmincke, 1993; Gurenko et al., 2006), and La Palma in particular (Day et al., 2009, 2010; Gurenko et al., 2009; Klügel et al., 2017), preserve evidence for significant geochemical heterogeneity, attributed to variable lithological heterogeneities embedded within the plume source mantle. Similar geochemical heterogeneities are well-described in most OIB lavas globally (e.g., Zindler and Hart, 1986; Hart et al., 1992; Hofmann, 1997), with unresolved questions including the length-scales of such heterogeneities and whether they are sampled within single eruptions. This latter question is particularly important, since most OIB geochemical studies typically utilize a limited number of lava samples, and rarely concentrate on obtaining timeseries data from singular eruptive events (e.g., Vlastélic et al., 2009; Bindeman et al., 2022). A major question that also remains concerns the mechanisms by which individual OIB eruptions are fed and supplied.

Studies of historical eruptions within the Canary Islands have focused on seismic crises (Torres-González et al., 2020; Fernández et al., 2021), monitoring of submarine eruptions such as at El Hierro in 2011 and 2012 (e.g., Carracedo et al., 2012, 2015; Martí et al., 2013; Longpré et al., 2014; Meletlidis et al., 2015), or the petrology and volcanic features of historic deposits such as the 1730-1736 Timanfaya event on Lanzarote (Carracedo et al., 1992), the 1705 eruption on Tenerife (Albert et al., 2015), and the 1949 and 1971 eruptions of the Cumbre Vieja (Klügel et al., 2000; Barker et al., 2015). The latter studies have demonstrated geochemically diverse lava compositions erupted along the Cumbre Vieja volcanic ridge and in La Palma in general, reflective of changes in magma chemistry relating to both mantle source composition and to magma differentiation processes below and within the island edifice (e.g., Day et al., 2009, 2010; Gurenko et al., 2009; Klügel et al., 2017). With few exceptions, modern study of past eruptions at OIB volcanoes has been hindered by prolonged basaltic eruptive activity that can result in the earliest deposits of those eruptions being covered by later volcanic products and obscuring the precise history of such eruptions (cf. Klügel et al., 2000). Furthermore, while historical eruptions on La Palma have been studied for their petrology, basic information on seismic events is not readily available (Longpré, 2021).

The 2021 La Palma eruption spanned from 19 September to 13 December and is the most significant recent eruption in the Canary Islands in terms of its volume (~0.2 km^3), duration (85 days), and the degree of material destruction it left in its wake, amounting to nearly €1 billion in damage (Global Volcanism Program, 2021; Carracedo et al., 2022; Copernicus, 2022) (**Fig. 1**). In this contribution new major and trace-element geochemistry of bulk rocks from lava samples collected throughout the 2021 eruption are reported along with bulk rock ^{187}Re-^{187}Os and highly siderophile element (HSE: Os, Ir, Ru, Pd, Pt, Re) abundance data, and olivine and clinopyroxene major, minor and trace element data for subsets of the lavas. Combined with seismic network coverage and precursor indications of volcanic unrest (Torres-González et al., 2020; Fernández et al., 2021), this new dataset provides an opportunity to understand plume-fed magmatism in the Canary Islands and to explore implications for the processes that trigger ocean island volcanic eruptions.

2. Sampling and methods

Systematic sampling was conducted throughout the entire eruption period to collect materials from newly emanated lava flows. This was an important research strategy since later lava emissions frequently covered tongues and lobes from earlier in the eruption, making them inaccessible for post-eruptive sampling. Samples were primarily curated at the University of La Palmas de Gran Canaria and the University of Barcelona, where they were cataloged, sawn, and distributed to consortium participants for further analysis. Detailed descriptions of the analytical methods employed in this study are provided in the *Supplementary Materials*. In brief, scanning electron microscopy (SEM) imaging of selected samples was conducted at the Swedish Museum of Natural History and the University of Freiburg, while X-ray fluorescence analysis of lavas was performed at the University of Barcelona. Bulk rock and mineral major-, minor- and trace-element abundance data and Os isotope and HSE abundance measurements were determined at the Scripps Isotope Geochemistry Laboratory at Scripps Institution of Oceanography using established methods. Olivine and clinopyroxene grains were separated from selected samples and analyzed by laser-ablation ICP-MS in 16 separate analytical sessions using a *New Wave* UP213 (213 nm) laser, coupled to a *Thermo Scientific* iCAPq Qc ICP-MS at the SIGL, with V-in-olivine determination performed using established methods (Nicklas et al., 2022a,b).

3. Results

Bulk rock major- and trace-element abundance data are reported for 47 selected lava samples (including four bombs) spanning the 85 days of the 2021 La Palma eruption (*Table S1*), along with petrology and mineral chemistry for a subset of these samples (*Tables S2, S3*). Lavas range in appearance from massive to highly vesicular (having up to 50% vesicles; **Fig. 2a**) are porphyritic and typically contain clinopyroxene + olivine + Fe-Ti oxide ± amphibole (kaersutite) grains <5 mm in length, set in a fine-grained to glassy groundmass consisting of microlites of clinopyroxene, plagioclase, olivine, magnetite, and sulfide (**Fig. 2c-e**). Earliest lavas were found to contain clinopyroxene (<7 mm, <20 vol%), olivine (<0.5 mm, ~5 vol%), partially reacted kaersutite (<10 mm, ~5 vol%) and minor Fe-Ti oxide crystals as well as small (<2 mm) partially reacted inclusions of gabbro (~1-2 vol%; **Fig. 2f,g**). Later lavas have a similar primary crystal cargo, although the presence of amphibole and gabbroic xenolith fragments diminished almost completely as the eruption progressed. In these later lavas olivine abundance (to 10 vol.%) and crystal size (typically to <1 mm) increased, while clinopyroxene remained relatively constant in terms of size and abundance. The primary crystal cargo also displays complex crystal textures, including zoned clinopyroxene grains (**Fig. 2h**), disequilibrium textures (sieve textures and reaction rims in amphibole; **Fig. 2f**), as well as skeletal growth of olivine in the earliest lavas. From the textural record it appears that several crystal textural populations exist for clinopyroxene and olivine, which require dedicated investigation to be resolved. Frothy, pale-coloured, silicic xenoliths known as "xeno-pumice" (cf. Troll et al., 2012) were found in tephra samples (**Fig. 2b**), but not as inclusions in lavas. Selected tephra and xeno-pumice from the 2021 eruption are reported in *Table S1* and in Carracedo et al. (2022) for comparison with lavas.

The 2021 La Palma lavas show a progressive change from tephrite to basanite compositions with an overall range of 4.8-6.4 wt. % $Na_2O + K_2O$, $Na_2O/K_2O = 2.46 \pm 0.05$, and with MgO contents between 5.7 and 8.4 wt.%. Late-stage bombs (LP21-93, -94) have higher MgO (10.3-11.3 wt.%) and Ni contents. Loss on ignition (LOI) values are low and negative (average = -0.6), likely due to minor oxidation of Fe^{2+} during analytical procedures and attesting to freshness of samples. There are notable trends in lava composition with time from 19 September 2021 (day zero) to early October, and then from early October to late November, followed by a final interval from early to mid-December 2021, with the last lava sampling dating from day 82 (December 10) in our collection. In the figures, lavas are grouped as day 1-20, day 21-50 and day 50> so that eruption details are apparent. Due to the similarity of lava compositions after day 20, the latter lavas will be referred

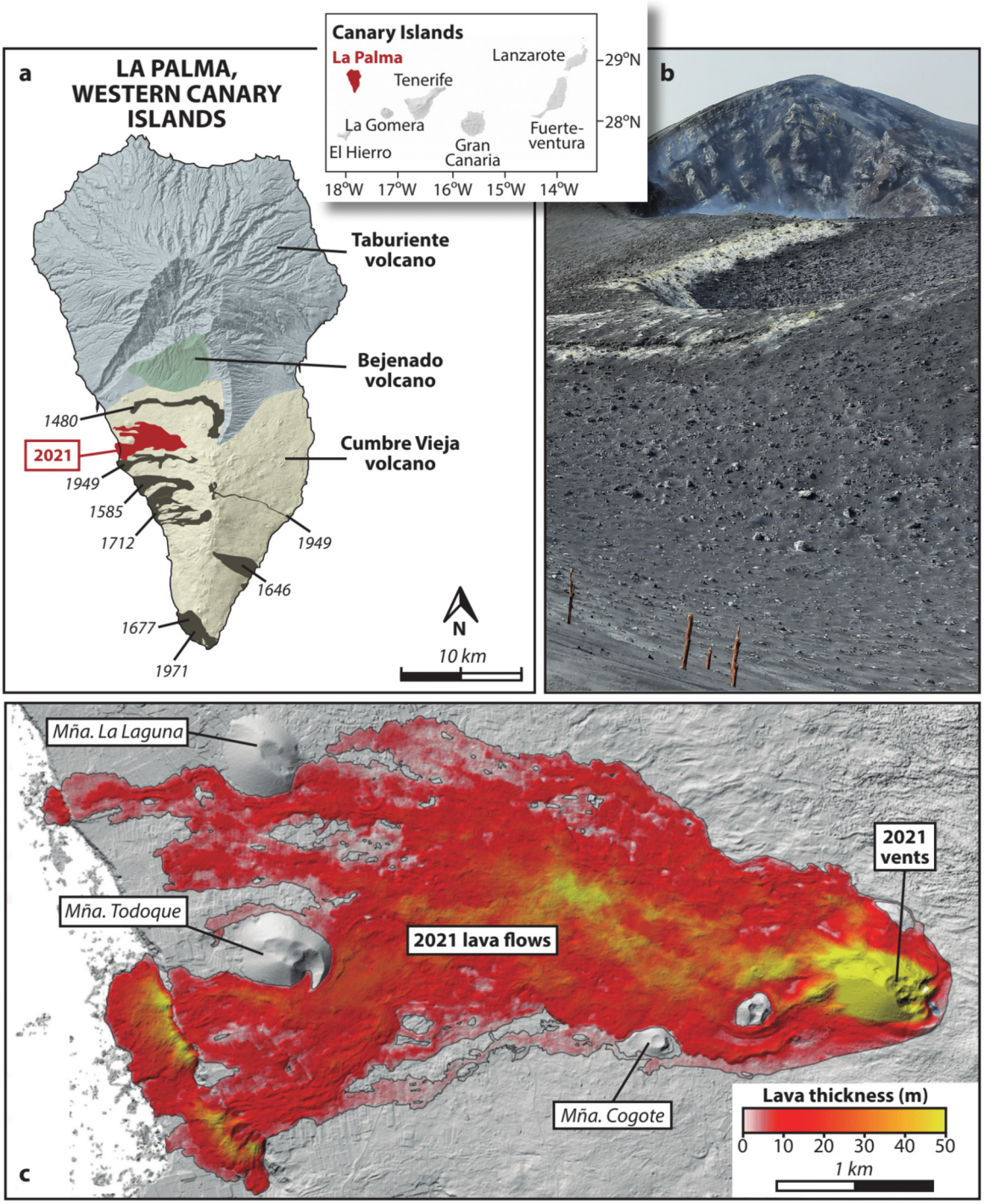

Fig. 1. Location maps of the 2021 La Palma eruption (inset and (a)) showing historic eruptions along the Cumbre Vieja volcanic ridge, image of eruptive vent complex after eruption termination (b), and lava flow thickness map (c). Total erupted volumes exceeded 0.2 km^3, covering an area of 12.25 km^2, equivalent to a time-averaged discharge rate of 27 m^3/s^{-1}. Shaded relief map in Fig. 1a is from GRAFCAN; Fig. 1c is adapted from Carracedo et al. (2022).

to together. General trends are relatively low MgO and compatible element (Cr, Ni) contents in the earliest lavas, with a progressive increase up to day 20, followed by 'plateauing' from day 21 to 70, with an irregular decrease up to day 85 (**Fig. 3** and *Figure S1*). Total alkalis, TiO_2 and incompatible trace elements, including the rare earth elements (REE), have the highest abundances in lavas from the start of the eruption and steadily decrease to around day 20. They then rise and plateau from day 21 to 82 with minor variations observed towards the end of the eruption. These changes in lava chemistry are also reflected in increases in bulk rock Mg-number, from ~46 to ~55, and CaO/Al_2O_3, from ~0.7 to ~0.9. Despite absolute decreases in incompatible element abundances for lavas from day 1-20, broadly flattening after day 21, primitive mantle normalized patterns are similar, with relative depletions in Cs, Rb, Ba, Th and U and strong negative Pb anomalies (*Figure S2*). Canonical OIB trace element ratios (Hofmann, 1997), including Ce/Pb (42.7 ± 3.2; 1 St Dev, n = 45), Sr/Nd (16.3 ± 1.1, n = 52), Th/U (3.6 ± 0.2) and Nb/Zr (0.27 ± 0.01) are relatively invariant throughout the duration of the eruption, whereas ratios such as La/Yb and Zr/Hf decreased during the first 20 days, then plateaued

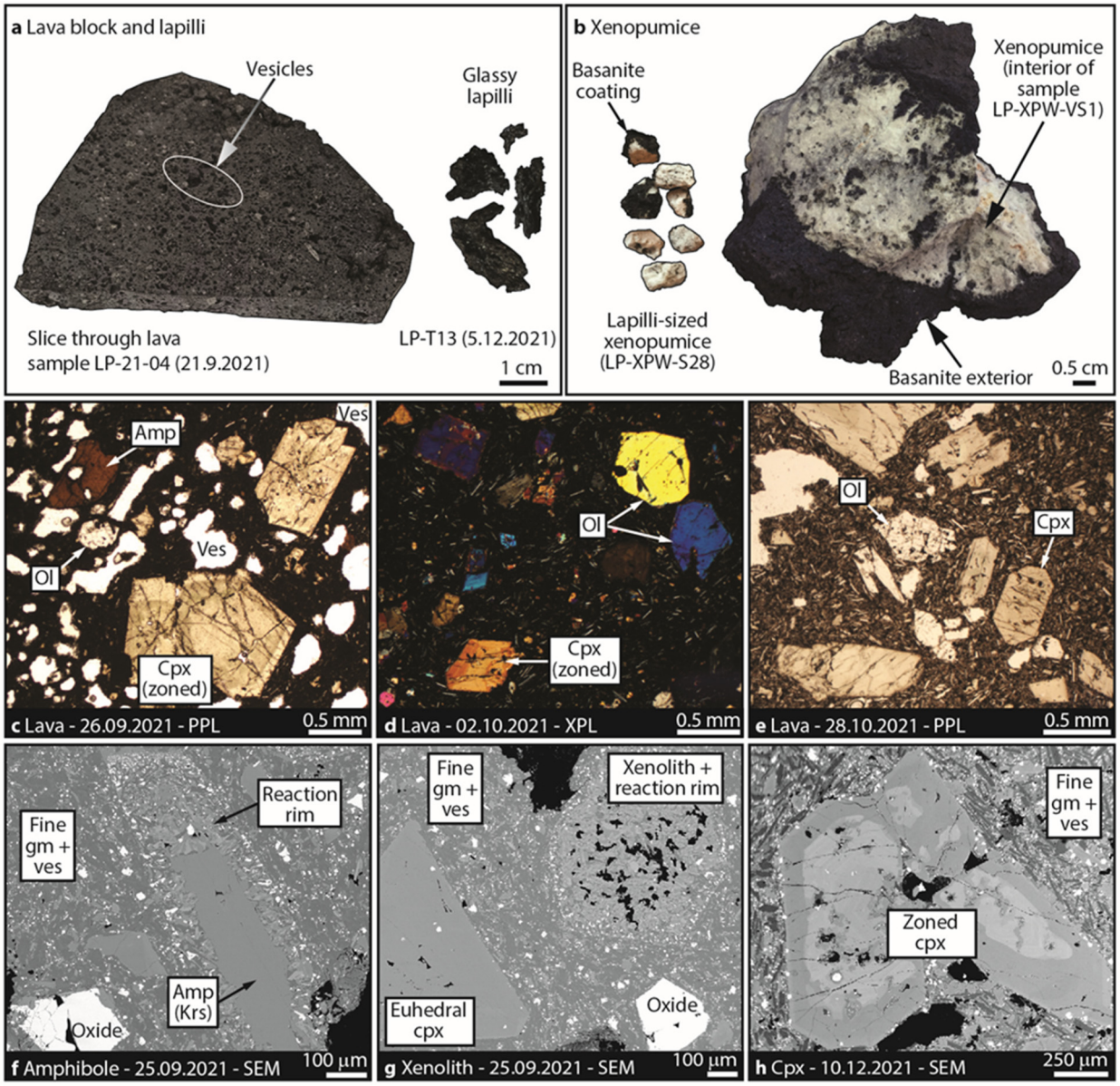

Fig. 2. Petrological features of the La Palma 2021 eruption. (a) Images of cut slice of LP21-04, erupted on 21st September 2021, along with glassy lapilli from December 2021; (b) xeno-pumice fragments and inclusions from the 2021 eruption; (c, d, e) plane polarized (PPL) or cross polarized light (XPL) images of various lava samples showing vesicles (Ves), olivine (Ol), clinopyroxene (Cpx) and amphibole (Amp); (f, g, h) back scattered electron (BSE) images showing complex reaction rims surrounding both kaersutite (Krs) crystals and xenolithic fragments (early lavas), oxides, and clinopyroxene all set in a fine groundmass (gm).

to about day 70, increasing again from late November/early December to the end of the eruption.

Fourteen samples were analyzed for Re-Os isotopes and highly siderophile element (HSE: Os, Ir, Ru, Pt, Pd, Re) abundances, spanning days 1-77 of the eruption (**Table 1**). Consistent with their behavior as compatible elements, concentrations of Pd, Pt, Ir and Os increase concomitantly with MgO, Ni and Cr. In turn, increases in Pd, Pt, Ir and Os are generally accompanied by decreases in $^{187}Re/^{188}Os$ and $^{187}Os/^{188}Os$ (**Fig. 4**; *Figures S3-S5*). Earlier erupted lavas have lower absolute HSE abundances and more fractionated HSE patterns than later erupted lavas (**Fig. 5**) but show absolute HSE abundances, similar to or lower than, the highest MgO lavas from the northern shield of La Palma (Day et al., 2010). Earlier erupted 2021 La Palma lavas have $^{187}Os/^{188}Os$ (0.143-0.148), which are generally more radiogenic than later erupted lavas and show steadily increasing Os contents from day 1 to 20, with a range from 5 to 51 ppt. Later erupted lavas contain between 23 and 89 ppt Os and, apart from two samples, have $^{187}Os/^{188}Os$ between 0.140 and 0.145. Sample LP21-68 from day 42 of the eruption has the highest reported Os content (89 ppt) and a $^{187}Os/^{188}Os$ ratio of 0.1363 that is unusually low for La Palma in general (Marcantonio et al., 1995; Day et al., 2009, 2010). Conversely, LP21-81 has 35 ppt Os and unusually radiogenic $^{187}Os/^{188}Os$ (0.1716). These outlying samples are discussed in more detail below.

Compositions of clinopyroxene broadly overlap in major-, minor- and incompatible trace-element abundances for day 1 to 20 and the >day 20 lavas (*Figure S6*). Calculated clinopyroxene equilibrium REE melt compositions using the values for McKenzie and O'Nions (1991) are elevated with respect to bulk rocks but have similar REE patterns (*Figure S7*). Olivine grains within the day 1 to 20 lavas have a limited range of average forsterite contents (molar $Mg/[Mg+Fe^{2+}]$; Fo_{79-81}; **Table 2**) and Ni (909 to 1246ppmw) compared with the day 21-50 (Fo_{80-84}; Ni = 1228 to 2207ppmw) and day >50 lavas (Fo_{80-83}; Ni = 1228 to 1369ppmw) (**Table 2; Fig. 6**). The parameter "X_{px}" ((0.001341 × (Ni) × (FeO/MgO))-0.437) can be used to express Ni enrichment at a given Fo number

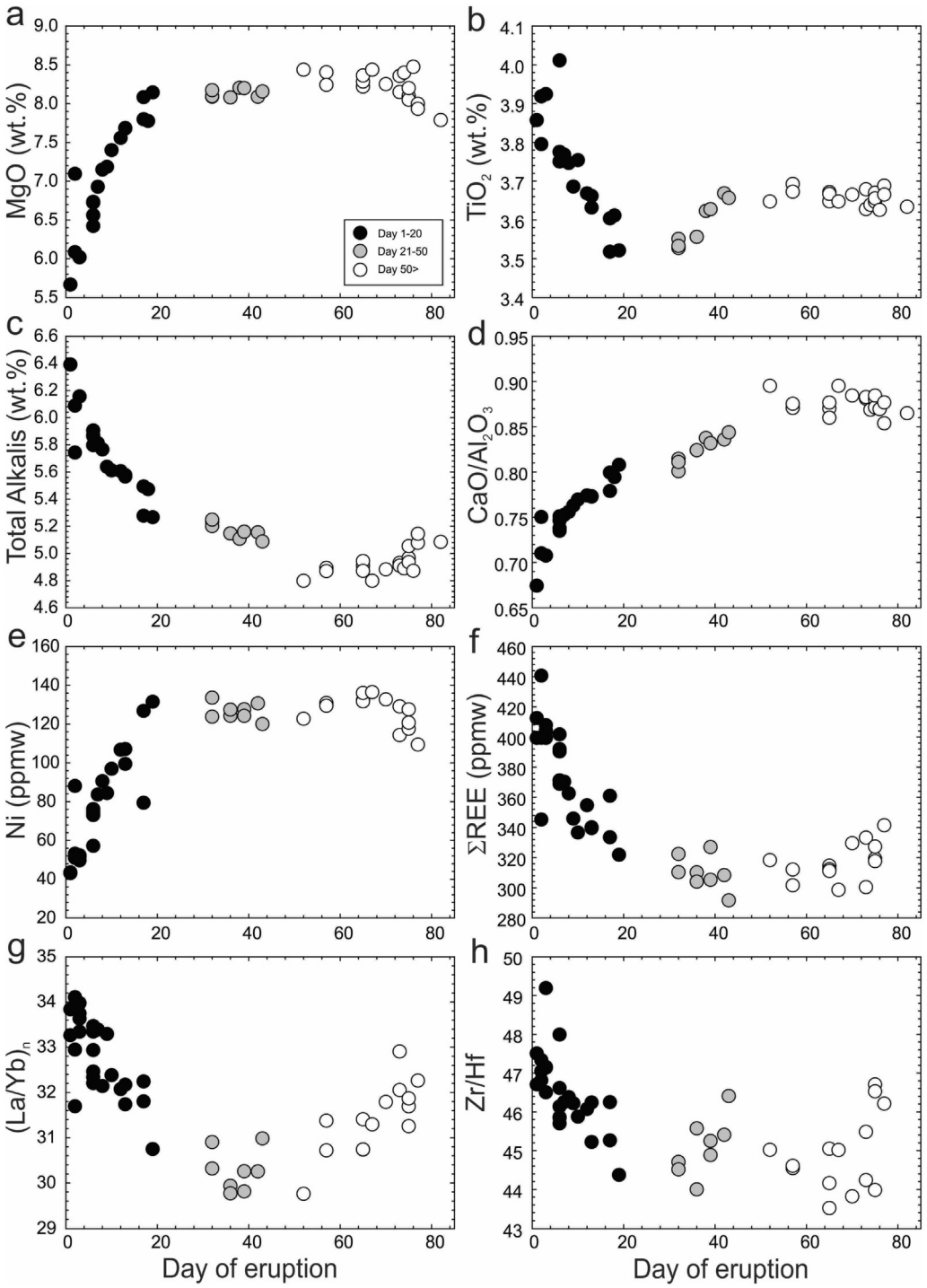

Fig. 3. Geochemical variations in lavas from the 2021 La Palma eruption as a function of the day of eruption, beginning on 19 September 2021. Variations shown are days of eruption versus (a) MgO, (b) TiO_2, (c) total alkalis ($Na_2O + K_2O$), (d) CaO/Al_2O_3, (e) Ni, (f) total rare earth element abundance, (g) La/Yb and, (g) Zr/Hf. Uncertainties on XRF and ICP-MS measurements are less than 2% relative and ~5% relative, respectively (see *Table S1*).

to determine the potential abundance of pyroxenite in the source (e.g., Sobolev et al., 2007). The X_{px} component in the La Palma 2021 eruption ranges between 0.15 and 0.6 with an average of 0.31 ±0.12 (1SD). Olivine grains have between 5.2 ±0.3ppmw and 7.2 ±2.4ppmw V, while bulk rocks have consistent V contents of 313 ±7ppmw. Calculated parental melts range between 7.1 and 9.5 wt.% MgO, with estimated eruptive temperatures of 1145 ±15°C, which is within uncertainty of measured lava eruption temperatures (~1140°C; PEVOLCA, 2021; Carracedo et al., 2022). Using the V-in-olivine oxybarometry technique (e.g., Wang et al., 2019; Nicklas et al., 2022a,b), fO_2 relative to the Fayalite-Quartz-Magnetite (FMQ) buffer can be calculated to be between +1.3 and +2 (**Fig. 7**). The moderate abundance of clinopyroxene (≤20 vol%) and other fractionated phases means that these are inconsequential within the estimated uncertainties of the V-in-olivine method (typically ±0.5 ΔFMQ; see Nicklas et al., 2022b for a detailed discussion). Although within analytical/procedural uncertainties, there is a hint of a negative correlation between olivine forsterite content and calculated fO_2; the data are otherwise consistent with the oxidized nature of western Canary Island lavas and OIB in general (Brounce

Table 1
Representative elemental and highly siderophile element abundances and Os isotopes of 2021 La Palma lavas.

	Day	MgO (wt.%)	Ni (ppm)	La/Yb_{PM}	Re (ppb)	Pd (ppb)	Pt (ppb)	Ru (ppb)	Ir (ppb)	Os (ppb)	$^{187}Re/^{188}Os$	2SE	$^{187}Os/^{188}Os$	2SE
LP21-02	1	*5.7*	*43*	*22.6*	0.680	0.176	0.254	0.294	0.027	0.005	618	13	0.1461	0.0009
LP21-12A	3	*6.0*	*52*	*23.1*	0.669	0.355	0.290	0.258	0.024	0.008	394	8	0.1483	0.0010
LP21-22	6	*6.4*	*57*	*22.4*	0.611	0.309	0.349	0.239	0.034	0.017	173	3	0.1451	0.0030
LP21-36	7	*6.9*	*84*	*22.7*	0.712	0.698	0.524	0.291	0.030	0.018	192	4	0.1439	0.0008
LP21-40	10	*7.4*	*97*	*22.0*	0.737	0.705	0.549	0.307	0.059	0.025	143	3	0.1435	0.0005
LP21-49	13	*7.7*	*107*	*21.9*	0.714	0.798	0.679	0.329	0.069	0.032	108	2	0.1442	0.0019
LP21-55	19	*8.1*	*132*	*20.9*	0.652	1.455	0.831	0.367	0.063	0.051	61.1	1.4	0.1428	0.0014
LP21-56	32	*8.1*	*134*	*20.6*	0.543	1.244	0.968	0.352	0.074	0.056	46.8	0.9	0.1431	0.0003
LP21-60	36	*8.1*	*124*	*20.4*	0.618	1.517	0.996	0.364	0.066	0.051	58.0	1.2	0.1445	0.0018
LP21-68	42	*8.1*	*131*	*20.6*	0.578	1.236	0.859	0.302	0.103	0.089	31.4	0.7	0.1363	0.0002
LP21-77	57	*8.4*	*131*	*21.4*	0.536	1.648	0.936	0.278	0.077	0.029	89.0	1.6	0.1449	0.0005
LP21-81	57	*8.2*	*129*	*20.9*	0.559	1.528	0.925	0.332	0.089	0.035	77.6	1.4	0.1716	0.0005
LP21-79	65	*8.4*	*136*	*20.9*	0.609	1.396	0.845	0.282	0.062	0.027	109	2	0.1452	0.0006
LP21-85	77	*8.0*	*109*	*22.0*	0.753	1.576	1.080	0.297	0.106	0.083	43.7	1.2	0.1405	0.0003

Table 2
Summary of olivine compositions for the La Palma 2021 eruption.

		Eruption Day	Mg#	Mg (ppm)	Al (ppm)	Ca (ppm)	V (ppm)	Mn (ppm)	Fe (ppm)	Co (ppm)	Ni (ppm)	Zn (ppm)	fO_2	(+)	(-)	Temp (K)	X_{Px}
LP21-04	*Av*	2	78.7	243497	353	2096	5.8	2177	151555	201	909	119	2.0	0.5	0.4	1431	0.15
(n = 8)	*2SD*		*1.6*	*25190*	*241*	*364*	*1.3*	*231*	*10713*	*10*	*223*	*12*					
LP21-24	*Av*	6	80.5	259129	384	2149	6.5	2018	144323	199	1246	118	1.6	0.8	0.6	1427	0.28
(n = 15)	*2SD*		*2.1*	*11184*	*553*	*316*	*2.5*	*354*	*22138*	*25*	*199*	*15*					
LP21-33	*Av*	6	80.4	252321	302	2095	6.1	1955	141007	197	1213	112	1.7	0.4	0.3	1431	0.26
(n = 9)	*2SD*		*1.4*	*20772*	*127*	*179*	*1.0*	*117*	*9696*	*12*	*86*	*15*					
LP21-54	*Av*	32	83.5	245368	355	1741	6.0	1389	111175	176	2207	94	1.5	0.3	0.3	1419	0.60
(n = 14)	*2SD*		*1.6*	*17993*	*268*	*289*	*0.8*	*259*	*11764*	*14*	*549*	*13*					
LP21-56	*Av*	32	81.6	263443	305	2201	6.3	1886	136608	191	1369	109	1.6	0.6	0.5	1388	0.30
(n = 9)	*2SD*		*1.9*	*29568*	*214*	*216*	*1.9*	*298*	*20399*	*15*	*236*	*11*					
LP21-60	*Av*	36	79.9	241104	289	1926	5.6	1907	139689	194	1242	115	1.9	0.3	0.3	1406	0.31
(n = 11)	*2SD*		*1.4*	*18829*	*265*	*268*	*0.8*	*187*	*12649*	*13*	*178*	*23*					
LP21-63	*Av*	39	80.2	251753	360	2015	7.2	2001	142061	199	1228	114	1.5	0.7	0.5	1401	0.28
(n = 14)	*2SD*		*3.0*	*34472*	*239*	*638*	*2.4*	*179*	*12298*	*16*	*183*	*22*					
LP21-78	*Av*	65	80.5	224724	261	1775	5.7	1758	124846	177	1207	103	1.9	0.7	0.5	1423	0.26
(n = 8)	*2SD*		*1.4*	*12095*	*90*	*253*	*1.9*	*99*	*7935*	*6*	*125*	*11*					
LP21-83	*Av*	75	83.2	247220	303	1752	7.1	1500	114701	176	1785	101	1.3	0.4	0.3	1426	0.42
(n = 9)	*2SD*		*0.6*	*18163*	*70*	*147*	*1.3*	*68*	*5989*	*11*	*112*	*11*					
LP21-84	*Av*	75	80.3	231397	273	1943	5.4	1808	130035	179	1179	104	2.0	0.4	0.3	1413	0.25
(n = 10)	*2SD*		*0.4*	*6436*	*111*	*100*	*1.0*	*55*	*3540*	*9*	*34*	*6*					
LP21-85	*Av*	77	81.2	238209	239	1773	5.2	1758	126827	179	1281	100	1.9	0.2	0.2	1434	0.27
(n = 10)	*2SD*		*0.4*	*7388*	*11*	*36*	*0.3*	*48*	*4671*	*7*	*33*	*4*					
Average 2021 La Palma (n = 117)			80.9	245288	311	1951	6.1	1832	132984	188	1351	108	1.7			1418	0.31
St-Dev			1.4	11414	46	172	0.6	229	12653	10	351	8	0.2			15	0.12
RSD			2%	5%	15%	9%	10%	12%	10%	6%	26%	8%	13%			1%	38%

Information on eruptive temperatures, fO_2 constraints and X_{px} calculations are given in the main text and supplementary information. Eruptive temperatures are reported in kelvin and were estimated from T (in °C) = 1000 +20($MgO_{parental}$) from Nisbet et al. (1993). These estimates are within uncertainty of the actual eruption temperatures of lavas observed at the surface (~1413K; Carracedo et al., 2022).

et al., 2017; Moussallam et al., 2019; Nicklas et al., 2022a,b; Taracsák et al., 2022).

Reported basaltic tephra data (*Table S1*) are from >day 20 of the eruption and have compositions similar to lavas erupted on or around the same days. By contrast, light and dark grey xeno-pumice observed to fall with tephra on day 37 (26 October 2021) are highly distinct in composition from lavas or basaltic tephra, with the grey xeno-pumice having compositions akin to Cumbre Vieja phonolite samples (e.g., Day et al., 2010; Turner et al., 2015), and light-colored xeno-pumices having compositions akin to xeno-pumice collected at El Hierro in 2011-2012 (Troll et al., 2012).

4. Discussion

Lavas erupted during the 2021 La Palma eruption show temporal variations in their bulk compositions, ranging from tephrite to basanite, as well as variations in their Os isotope ratios and HSE abundances. Over the 82-day period of lava emission that was sampled, the most significant compositional variations occurred in the first 20 days, while other features of the lavas such as estimated parental melt compositions, eruption temperatures and fO_2 remained largely relatively uniform from days 20 to 70, with some additional variation after day 70. These features are now discussed considering possible variations in OIB lava chemistry during singular eruptive events and in the context of possible triggers for volcanic activity such as observed on La Palma in 2021.

4.1. Parental melt compositions and constraints on mantle source

A key question arising from the observed variations in the 2021 La Palma lavas is whether the eruption was fed by a homogeneous parental melt that experienced subsequent differentiation or from a heterogeneous mantle source. Previous studies of Canary Island lavas have proposed that distinct mantle sources fed volcanism within and between the islands based on radiogenic and stable isotope variations (e.g., Hoernle and Schmincke, 1993; Day et al., 2009, 2010; Gurenko et al., 2009). On the other hand, relatively restricted isotopic variations at La Palma might suggest a broadly homogeneous mantle source beneath the island (Marcantonio et al., 1995; Day et al., 2010; Klügel et al., 2017).

Despite major element compositional differences between the earliest and latest erupted lavas, estimated parental melt compositions (8.2 ±0.8 wt.% MgO; *Supplementary Information*) from olivine-bulk rock equilibrium relationships are relatively invariant and incompatible trace element abundances are broadly similar throughout the eruption (*Figure S2*). Even with minor variations in ratios of the REE (e.g., La/Yb), the estimated partial melting required from REE models can account for this variation and implies a relatively consistent 2.5 to 3% partial melt of a fertile asthenospheric man-

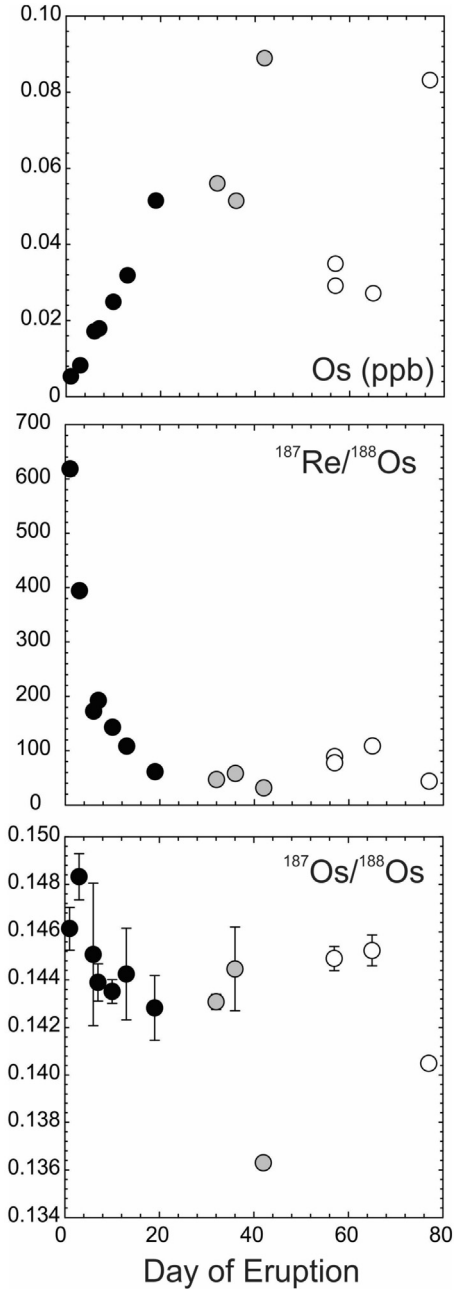

Fig. 4. Plots of (from top to bottom) Os concentration, $^{187}Re/^{188}Os$ and $^{187}Os/^{188}Os$ for lavas as a function of their eruption date. Full relationships for the HSE versus eruption date and MgO are given in the *Supplementary Information*. Analytical uncertainties on Os abundance are <0.5%, conservative uncertainties on $^{187}Re/^{188}Os$ are ±5% and uncertainties for $^{187}Os/^{188}Os$ include in run uncertainties. Error bars are shown or are smaller than symbols. Note, sample LP21-81 ($^{187}Os/^{188}Os$ = 0.1716) is not shown in the lower panel for clarity. Symbols as in Fig. 2.

tle source. These partial melts would have formed predominantly in the garnet stability field (**Fig. 8**), consistent with the thick (90-95 km) Jurassic-aged oceanic lithosphere beneath La Palma (Winterbourne et al., 2009). Similarities in parental melt composition extend to broadly consistent V-in-olivine estimates of fO_2 for the eruption. From a major and trace-element compositional perspective, both in bulk rocks and minerals, the 2021 La Palma eruption was therefore likely to have been fed by a homogeneous parental magma composition, varying only to a small degree in the potential depth and degree of partial melting.

Olivine compositions from the 2021 La Palma lavas display significant overlap, with the most forsteritic, Ni-rich olivine found in a

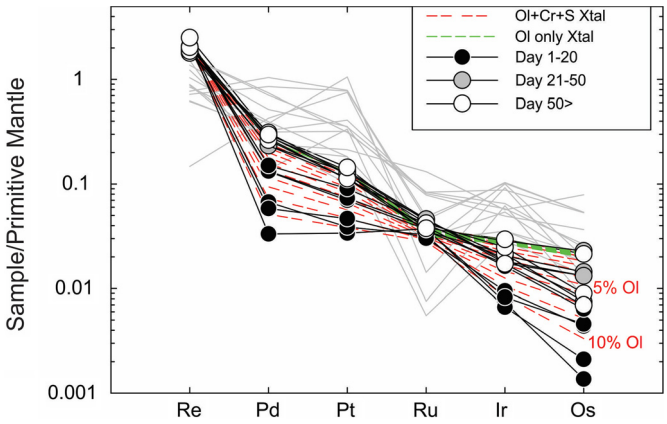

Fig. 5. Primitive mantle normalized highly siderophile element diagram showing lavas for the 2021 La Palma eruption versus HSE patterns for pre-historic Taburiente and Garafia shield stage lavas with 7.9 to 15.5 wt.% MgO from the north of La Palma from Day et al. (2010) (grey lines). Shown are two crystallization models; the first assumes only olivine crystallization (Ol only Xtal; green lines) from 0-10% olivine fractionation. The second model (Ol+Cr+S Xtal; red lines) shows the results for 0-10% olivine crystallization with co-crystallization of Cr-spinel and sulfide, in the proportions 0.98 olivine, 0.019 Cr-spinel, 0.001 sulfide, using the partition coefficients compiled in Table 4 of Day (2013). Primitive mantle normalization from Day et al. (2017). (For interpretation of the colors in the figure(s), the reader is referred to the web version of this article.)

day 20-50 lava (sample LP21-54; **Fig. 6**). The olivine compositions are generally more evolved than previously studied picro-basalts from La Gomera and La Palma (Gurenko et al., 2009), although some of the more forsteritic olivine grains have high Ni and low Ca, similar to some previously examined El Hierro and Tenerife high-MgO basalts. The X_{px} parameter (= 0.31 ±0.12) would imply the possibility of a pyroxenitic component in the 2021 La Palma magma source, and compositions of the lavas trend towards a pyroxenite endmember as suggested for Koolau (Hawaii; Sobolev et al., 2007). This component has been interpreted to originate from a primary peridotite source that converted to pyroxenite by solid-state reaction with recycled crust (X_{px} = ~0.35; Gurenko et al., 2009), which would be consistent with the oxidized compositions of the 2021 La Palma lavas and the general HIMU-type compositions of La Palma lavas (Gurenko et al., 2009; Day et al., 2010). Notwithstanding, deficiency in SiO_2 coupled with high alkalis, H_2O and CO_2 in basanitic melts make interpretation of a depleted olivine-pyroxenite (Gurenko et al., 2009), or enriched pyroxenite source for La Palma lavas (Day et al., 2009) based on olivine chemistry alone, ambiguous (Herzberg, 2011). Olivine-free mantle sources are not the sole means for generating Ni-rich olivine in OIB, with Ni and/or Fe/Mg diffusion (Lynn et al., 2017), crustal processing (Gleeson and Gibson, 2019) and average depths and extents of polybaric melting also likely to play a role in modifying Ni contents. From the perspective of the 2021 La Palma eruption, the presence of high-Ni olivine in some, but not all, of the lavas implies both autocrysts and antecrysts co-exist in samples.

It has been shown that La Palma lavas, especially those from the Cumbre Vieja, span a relatively narrow range of Sr-Nd-Pb isotope compositions ($^{87}Sr/^{86}Sr$ = ~0.70306-0.70318; $^{143}Nd/^{144}Nd$ = 0.51288-0.51290; $^{206}Pb/^{204}Pb$ = 19.5-19.8; Day et al., 2010; Klügel et al., 2017), but show a wide range of $^{187}Os/^{188}Os$ compositions (0.138-0.174; Marcantonio et al., 1995; Widom et al., 1999; Day et al., 2009, 2010) for lavas with >50 ppt Os. Osmium isotope ratios for the 2021 La Palma eruption (0.1363 to 0.1716) span almost the entire range of $^{187}Os/^{188}Os$ previously reported for La Palma. While source heterogeneity for the most extreme Os isotopic variations cannot be entirely excluded, the prevalent trend in $^{187}Os/^{188}Os$ is for a general decrease from more radiogenic values at the start of the eruption to lower ratios towards the end. Omitting the most

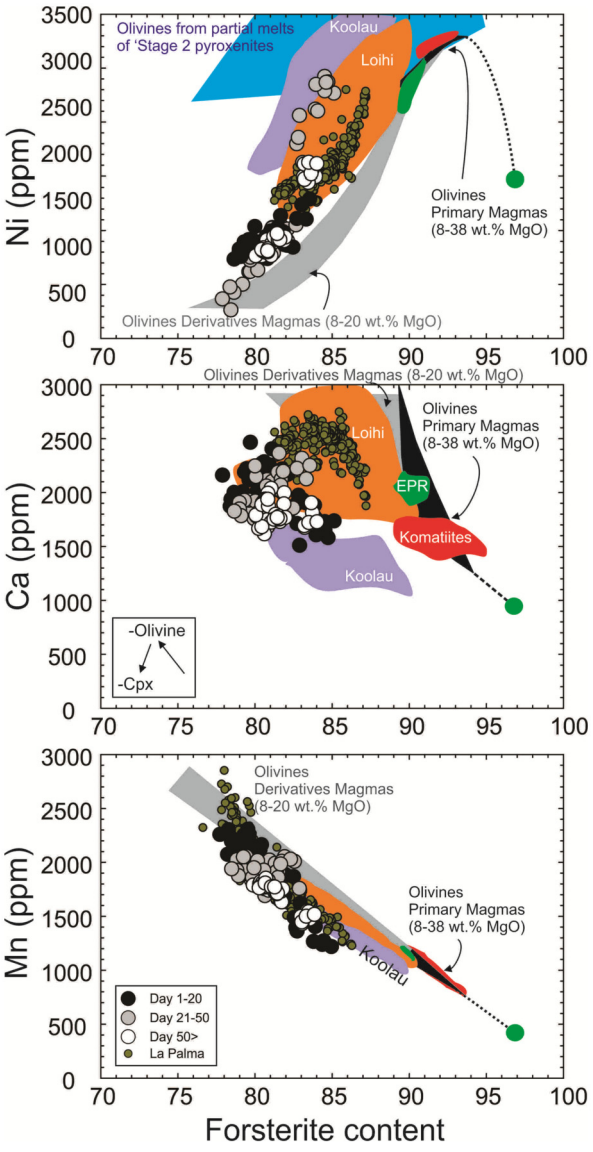

Fig. 6. Compositions of 2021 La Palma lava olivine grains obtained by LA-ICP-MS versus olivine from high MgO basaltic rocks from La Palma, El Hierro, La Gomera and Tenerife (Gurenko et al., 2009), and compositional fields of Koolau and Loihi (Hawaii), Sequeiros mid-ocean ridge basalts from the East Pacific Rise (EPR), and Alexo komatiites (Herzberg, 2011) showing primary olivine compositions and derivative olivine compositions from evolving magmas relative to a peridotite composition (green circle) and to estimated compositions of olivine derived from partial melts of a (stage 2) pyroxenite (Herzberg, 2011). Forsterite contents are accurate and precise to better than 2.5% using this method (see *Supplementary Information*).

(sample LP21-81) and least (sample LP21-68) radiogenic samples (discussed below) gives an average $^{187}Os/^{188}Os$ of ~0.1443 ±38 (n = 12; 2SD) that is close to the typical $^{187}Os/^{188}Os$ measured in La Palma alkali basalts with >50 ppt Os (~0.145; Marcantonio et al., 1995; Widom et al., 1999; Day et al., 2009, 2010). The Os isotope compositions of La Palma lavas have been interpreted to reflect radiogenic contributions from relatively young HIMU-type recycled oceanic lithosphere (Day, 2013). Based on the Os isotope and major and trace element data, there is no compelling reason to suggest significant changes in parental melt composition with time, with the 2021 La Palma lavas originating from a mantle source typical of Cumbre Vieja and many La Palma lavas, in general, supporting a broadly homogeneous mantle source.

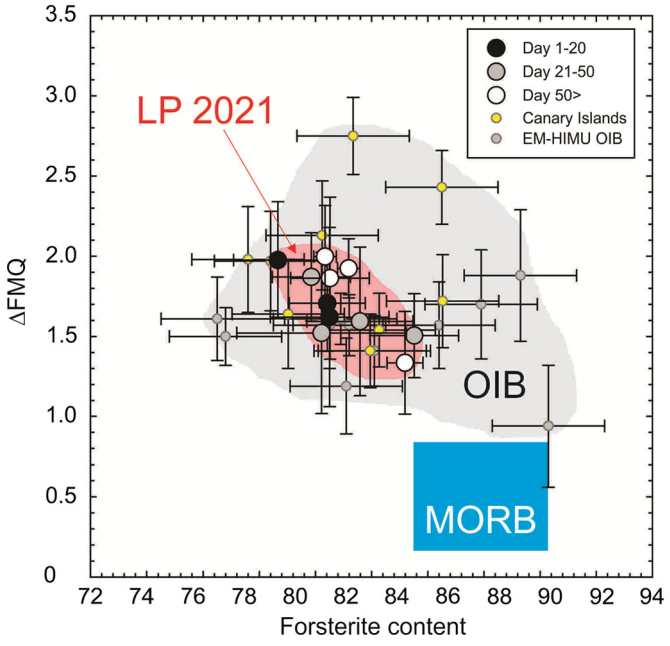

Fig. 7. Forsterite contents and oxygen fugacity estimates, in log units relative to the fayalite-magnetite-quartz (FMQ) redox buffer, using the V-in-Olivine oxybarometer for the 2021 La Palma eruption. Previously published Canary Island lava and other ocean island basalt (OIB) data are from Nicklas et al. (2022b), with the MORB estimate from Nicklas et al. (2019) assuming Siqueiros fracture zone olivine forsterite compositions.

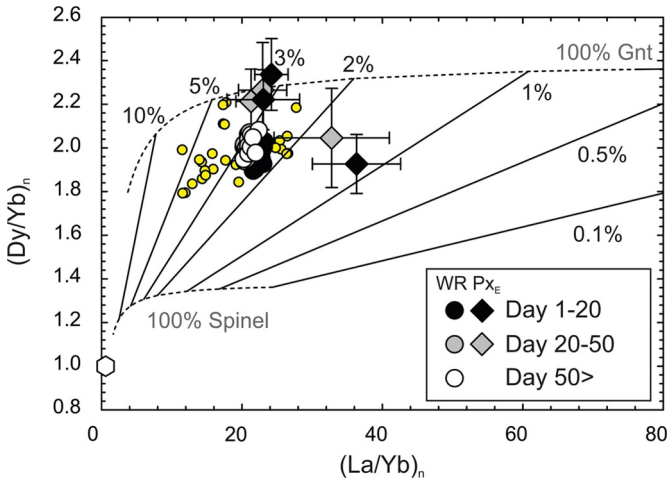

Fig. 8. Estimates of partial melting for 2021 La Palma lavas versus previous La Palma lavas (yellow circles; Day et al., 2010) and typical N-MORB composition (unfilled hexagon). The model assumes a primitive mantle source (McDonough and Sun, 1995) with garnet (Gnt) peridotite starting modal proportions of olivine, orthopyroxene, clinopyroxene, and garnet of 0.598/0.211/0.076/0.115 and a spinel peridotite with olivine, orthopyroxene, clinopyroxene, and spinel of 0.578/0.21/0.119/0.033, with melting and partitioning phases equal to that given in McKenzie and O'Nions (1991). The black and grey diamonds are average parental melts estimates calculated from pyroxene compositions measured by LA-ICP-MS for the September and October eruptive products.

4.2. Fractionation of early magmas

Given arguments for limited parental melt compositional variations, the differences in final erupted lava compositions likely reflect differentiation processes that acted on early erupted lavas prior to eruption versus more primitive lavas emitted later in the eruption. Earliest erupted lavas have compatible (e.g., MgO, Ni) and incompatible (e.g., TiO_2) abundances suggestive of crystal-liquid fractionation that is broadly consistent with removal of olivine ±

clinopyroxene (± amphibole) ± spinel (**Fig. 3**; *Figure S1*). Day 1-20 lava compositions also approach the 'tipping point' in Harker diagrams where magnetite crystallization would be expected, and lava compositions would ultimately extend to phonotephrite (cf. Klügel et al., 2017, 2022). These relationships permit quantification of olivine crystallization required to form the earliest melts. Between 5 and 10% olivine crystallization can explain bulk rock compositions of earliest erupted lavas compared with a primitive parental melt composition estimated from olivine-bulk rock equilibrium and the most forsteritic olivine (Fo_{83-84}) measured during the 2021 La Palma eruption.

Assuming melts traversed through the same magma reservoir, then the progressive change from tephrite on day 1 of the eruption to basanite by ~day 20 of the eruption enables an estimate of potential magma storage volume and the amount of olivine that crystallized. Assuming that volcanic effusion rates (~27 m^3/s; IGN, 2022) for the duration of the eruption correspond to magma intrusion rates, then the approximate size of a magma chamber being replenished completely with magma in ~20 days would be approximately 0.02 km^3. Assuming 5-10% olivine crystallization for the earliest lavas would imply approximately 1 to 2 × 10^6 m^3 of olivine crystallization during significant cooling and segregation from their parental melt.

Changing major element compositions of lavas correspond with changes in incompatible trace elements. Most striking are variations in the compatible trace elements, including Ni and Co, but also the HSE. Partitioning between the HSE and olivine, Cr-spinel, sulfide and other crystallizing phases in basalts has been empirically determined (e.g., Day, 2013) and can be used to model variations in these elements for the 2021 La Palma eruption. For modeling, it was assumed fractionation was driven by crystallization of olivine in equilibrium with the most primitive melt (Fo_{83-84}) and using the day >50 lavas as the initial HSE content of the parental melt, since they are relatively unfractionated. Two sets of bulk partition coefficients were applied to the models: solely olivine crystallization (pyroxene partition coefficients are similar to or lower than olivine) and mixtures of olivine, Cr-spinel and sulfide crystallization. Even at an extreme of 10% olivine fractionation, more fractionated day 1-20 lava HSE compositions cannot be explained by crystallization of this phase alone. Better fits come from mineral assemblages where a maximum of 10% olivine (±clinopyroxene ±amphibole) is fractionally crystallized with proportions of 0.98 olivine, 0.019 Cr-spinel and 0.001 sulfide (**Fig. 5**). The HSE support crystallization of an olivine (±clinopyroxene ±amphibole)-dominated assemblage, but with minor spinel and sulfide co-crystallization. These results are consistent with the onset of sulfide saturation prior to the onset of magnetite saturation in 2021 La Palma lavas, evident from the lack of inflection of Ti and Fe on Harker diagrams (e.g., *Figure S1*).

4.3. Evidence for crustal and non-systematic contamination effects

In contrast to systematic HSE abundance behavior in most of the La Palma 2021 lavas, two samples measured for Os isotopic compositions are anomalous. LP21-68 from day 42 of the eruption had the highest reported Os content (89 ppt) and a $^{187}Os/^{188}Os$ ratio of 0.1363, whereas LP21-81 had 35 ppt Os and unusually radiogenic $^{187}Os/^{188}Os$ (0.1716). These features are not analytical artifacts (*Supplementary Information*). Radiogenic Os isotope compositions in OIB with <50 ppt Os are not uncommon and have been variably attributed to susceptibility of low Os lavas to crustal assimilation (e.g., Reisberg et al., 1993; Widom et al., 1999; Day, 2013). Conversely, some 2021 La Palma lavas have Os contents much lower than LP21-81 yet have less radiogenic $^{187}Os/^{188}Os$. OIB lavas with high Os contents and less radiogenic $^{187}Os/^{188}Os$ than associated low Os content lavas have often been explained through assimilation of less radiogenic lithospheric mantle components (e.g., Day, 2013). Although such possibilities cannot be completely excluded for 2021 La Palma lavas, the otherwise consistent and coherent geochemical features of the bulk of the lavas suggest such processes are unlikely. Variations in $^{187}Os/^{188}Os$ in LP21-68 and LP21-81 due to mantle source variations are also unlikely based on arguments for an invariant mantle source composition for 2021 La Palma parent magmas.

A feature of the 2021 La Palma eruption is that many of the lavas flowed across manufactured structures, including buildings with metal support and banana plantations that use metal frames to cover the plants, in addition to vehicles, fences, road signs and other contemporary infrastructure. Addition of small quantities of these materials into lavas has the potential to modify Os isotope signatures. For example, steel implements can contain significant Os contents (>50 ppb) with $^{187}Os/^{188}Os$ of <0.13 (Day et al., 2018) and it has been determined that anthropogenic pollutants can have both radiogenic and unradiogenic $^{187}Os/^{188}Os$ (Koushelar et al., 2021). Regardless of potential causes of the 'non-systematic' $^{187}Os/^{188}Os$ behavior for LP21-68 and LP21-81, a systematic relationship is evident in the lower Os contents, more radiogenic $^{187}Os/^{188}Os$ and higher $^{187}Re/^{188}Os$ in the earliest erupted 2021 La Palma lavas (**Fig. 4**). These variations can be attributed to crustal assimilation effects. In this regard, it is notable that lapilli falling on 26 October at La Palma contained occasional fragments (~<1 fragment of cm^2 per m^2 or ~<0.1%, based on field estimation) of xeno-pumice. Similar xeno-pumice materials have been found in numerous Canary Island eruption deposits, most notably the 1585 Roques de Jedey/Tehuya lavas (Carracedo and Troll, 2016) and the 2011 El Hierro eruption (Troll et al., 2012; Meletlidis et al., 2012; Zaczek et al., 2015), and have been attributed to formation from evolved phonolite lithologies and from Jurassic or younger sedimentary material from the Atlantic Ocean floor that have been assimilated into magmas during their ascent (Hoernle, 1998; Hansteen and Troll, 2003; Carracedo and Troll, 2016). The 2021 La Palma white xeno-pumice has high SiO_2 (~72 wt.%) and low Sr, being similar in composition to some ocean floor siliceous sediments (Carracedo et al., 2022; *Supplementary Tables*). Grey xeno-pumices have moderate SiO_2 (~54 wt.%) and high Rb, Sr, Zr, Pb, U and Th, consistent with La Palma phonolite compositions (cf. Day et al., 2010; Klügel et al., 2017). Xeno-pumice fragments provide incontrovertible evidence for minor assimilation of sedimentary and volcanic edifice materials into magmas and point to the potential for contamination within the underlying oceanic crust and lithosphere. While this assimilation has a limited influence on lava major- and trace-element compositions, assimilation and fractional crystallization processes probably led to low Os contents, higher Re/Os and inheritance of radiogenic $^{187}Os/^{188}Os$ in some of the day 1-20 lavas.

4.4. Geochemical and geophysical constraints on the 2021 La Palma eruption

Seismic detection, gas monitoring and geodetic surveys of La Palma noted magmatic unrest since October 2017, with accelerated unrest in early September 2021, preceding the eruption itself (Torres-González et al., 2020; Fernández et al., 2021; Longpré, 2021; Carracedo et al., 2022). Pre-eruptive seismic events occurred at 15 to 30 km depth and have been interpreted to reflect the earliest unrest associated with the eruption (Fernández et al., 2021). This likely represents the period of initial magma emplacement leading up to the 2021 La Palma eruption. Between October 2017 and August 2021, earthquake depths generally increased from 20-25, to 30-35 km depth and were of limited magnitudes (1-2), with typical depths between 20 and 30 km. From 8 to 11 September 2021 there was a pronounced shift in earthquake depths to 8-14

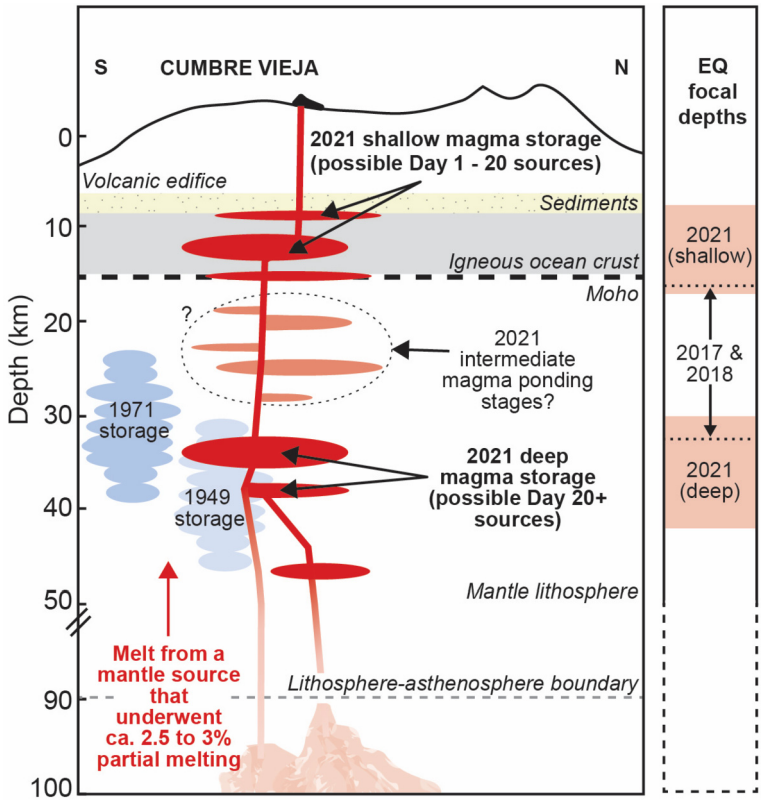

Fig. 9. Conceptual model for the magma plumbing system beneath La Palma in 2021, versus magma storage depths for the historical 1949 and 1971 eruptions. Parental magmas originated from ca. 2.5-3% partial melting of an asthenospheric mantle source. Initial magmas migrated to <40 km in late 2017 where they fractionated olivine ± clinopyroxene + Cr-spinel + sulfide prior to eventual mobilization in September 2021. As the eruption progressed, progressively deeper portions of the underplating magma feeding zone were involved in the eruption. Shown are the barometry estimates for crystallization pressures for the La Palma 1949 and 1971 eruptions from Klügel et al. (2000) and Barker et al. (2015), a potential intermediate magma ponding zone based on fluid inclusion depth estimates from Zanon et al. (2022), and earthquake (EQ) focal depths data summarized from the IGN (2022).

km, and progressive shallowing from 6 km to the surface on 19 September, when the eruption commenced (Global Volcanism Program, 2021) (*Figure S8*). After 19 September, earthquake locations were generally between 8 to 17 km and from the beginning of October also at 30 to 40 km beneath the volcano (IGN, 2022), where the largest earthquakes occurred in the deeper regions, and with increased magnitudes, reaching up to magnitude 5 from October to early December, 2021. Earthquake activity subsided in intensity after a particularly intense episode in late November to early December (IGN, 2022; Carracedo et al., 2022), which coincides with some minor variations of major and trace element composition in the lavas erupted during approximately the last two weeks of the eruption.

The general depth of 2017-2021 earthquake foci match with prior barometry and petrological studies of pre-historic (Galipp et al., 2006; Klügel et al., 2022) and historic lavas where robust seismic data were not available. For the 1949 and 1971 eruptions of La Palma, for instance, both deep (25-45 km; Klügel et al., 2005; Barker et al., 2015) and shallow (10-15 km; Klügel et al., 2000) magma chambers have been proposed, with a possible degree of shallowing of the magma storage system between the 1949 and 1971 eruption events (Barker et al., 2015) (**Fig. 9**). For the 1949 eruption, magma intrusion and fractionation of melts has been proposed to have occurred as early as 13 years prior to the eruption itself, and the opening of three separate vents led to the emplacement of magma compositions ranging from basanite to phonotephrite (Klügel et al., 2000). Previous work has shown that recent La Palma volcanism is charged by rift-oriented dikes running approximately north-south along the dorsal ridge of the Cumbre Vieja (Carracedo et al., 2001), a feature characteristic of rift-fed volcanism in the Canary Islands in general (Carracedo and Troll, 2016). Initial magma migration and emplacement in the underplating zone could have been as early as 2009 or 2010 (Fernández et al., 2021), with larger volume magma migration reflected in the seismicity of 2017 to 2020 beneath La Palma. This pre-cursor unrest can now be interpreted to reflect the injection of magma from dykes into the main reservoir zones at 8-40 km depth, where parental magmas underwent crystal-liquid fractionation processes, ultimately producing compositions from early fractionated tephrite to more primitive basanite. This is consistent with preliminary fluid inclusion results that imply a somewhat shallower origin for the tephrites (ca 17 to 8 km) than for the basanites ($\geq$ 26 to 22 km; Zanon et al., 2022). While there is limited seismic evidence for magma supply from below >50 km from September to December 2021, we consider that recharge of primitive melts from greater depth could nevertheless have played a role during the eruption, but this suggestion awaits further testing.

The 2021 eruption has led to larger volumes of volcanic material being emplaced than for any prior historical eruption on La Palma (Carracedo et al., 2022; González, 2022). The compositional evolution of the lavas and tephras from a more evolved tephrite composition to more primitive basanite follows a similar progression to the 1949 eruption (cf. Klügel et al., 2000). In the case of the 2021 La Palma eruption, earliest indications for magma migration from surface deformation happened some 10 years prior to volcanism (Fernández et al., 2021), with seismic activity becoming more pronounced some four years prior to eruption (*Figure S8*). In the case of the 1949 eruption, and to a lesser degree now also the 2021 eruption, the longevity of magma storage beneath the volcano led to significant fractionation of melts to tephriphonolite

in 1949 and to tephrite in 2021. It appears that even longer-term storage likely leads to the formation of phonolitic compositions beneath La Palma (cf. Klügel et al., 2017, 2022). For the 2021 eruption, exhaustion of the most evolved products within the upper parts of the underplating zone was associated with earthquakes dominantly at 8 to 17 km within the first two weeks of the eruption, succeeded by progressively more primitive magmas erupting from late October to late November associated with intense additional deep earthquake activity at ~30-40 km depth (**Fig. 9**). This main sequence of events was followed by a slightly more variable range of compositions in early to mid-December, which started after the major earthquake events of late November to early December (IGN, 2022). After this, earthquake activity and lava emission rates generally subsided until the end of the eruption on December 13th 2021.

4.5. Implications for OIB sampling and eruptions

The 2021 eruption of La Palma has provided a wealth of knowledge on volcanic monitoring of unrest, hazard management, and now also petrological information (Longpré, 2021; Pankhurst et al., 2021; Carracedo et al., 2022; González, 2022). It will doubtless provide more insights on OIB volcanism as the enormous quantities of data collected during the eruption are processed and understood. From the perspective of the petrology and geochemistry of the lavas, we highlight two critical lessons from the eruption. First, time-series sampling of lavas demonstrates significant changes in chemistry, including evidence for crystal-liquid fractionation and crustal contamination. Such observations are not possible from studies that collect single samples from individual OIB eruptions (e.g., Day et al., 2010). Instead, detailed studies of individual eruptions at La Palma (e.g., Klügel et al., 2000; Barker et al., 2015) and elsewhere (e.g., Vlastélic et al., 2009; Bindeman et al., 2022) serve a valuable and complementary purpose to more general geochemical studies. Whereas the former types of studies can only provide a snapshot of conditions, but are important for addressing mantle sources and mantle heterogeneity, the latter provide key information on eruption progression and allow tests for small-scale mantle heterogeneities versus magmatic differentiation processes. Indeed, dedicated studies of the 1949 and 1971 eruptions of the Cumbre Vieja of La Palma suggest that they share many similarities to the 2021 eruption, which is an important finding with respect to hazard prediction (**Fig. 9**). The presented results also show the power and utility of Os isotope and HSE abundance measurements in studying individual eruptions such as that on La Palma, due to the low Os contents that can occur in fractionated lavas to enable recognition of crustal contamination effects.

The second and perhaps most critical aspect of the geochemistry and geophysical conditions of the 2021 eruption are the evidence for magma migration and magma storage up to several years preceding the eruption leading to initially fractionated tephrite compositions, to later more primitive basanitic magmas. These observations suggest that, in the absence of magma recharge events, magmas can stall and fractionate to relatively evolved compositions, even to phonolite, in the case of La Palma (cf. Turner et al., 2015; Klügel et al., 2017, 2022). In this sense, magmatism on La Palma shows similarities, albeit at smaller-scale, to larger silicic systems, where either long-term cold or warm (e.g., Cooper and Kent, 2014; Bachmann and Huber, 2016; Cashman et al., 2017) magma storage is responsible for differentiation and can lead to compositionally zoned eruption deposits. In the case of La Palma, this process occurred at least three times in the last century (1949, 1971, 2021) and resolving whether this is also a driving force for other alkali basalt dominated ocean islands with active volcanism, such as the Azores, will be important to understand. Another potential puzzle lies in the relatively low calculated MgO contents of parental melts for the 2021 eruption, and for historical Cumbre Vieja lavas in general. These compositions are generally much less magnesian than for shield-stage lavas from the northern shield of La Palma, or shield stage phases for Gran Canaria or Tenerife (cf. Gurenko et al., 2006, 2009; Day et al., 2010; Klügel et al., 2017). Understanding whether this might reflect waning of shield stage magmatism in La Palma or instead indicate the partial melting of a relatively volatile-rich mantle source possibly dominated by an unusual lithological component (i.e., pyroxenite) beneath the Cumbre Vieja volcanic ridge, remain outstanding questions.

5. Conclusions

The 2021 Cumbre Vieja eruption of La Palma allows for examination of magmatic processes during a rift zone eruption of an OIB volcano. Over the course of the eruption, lava temporal changes from tephrite to basanite and from more to less radiogenic $^{187}Os/^{188}Os$ demonstrate initial eruption of chemically fractionated lavas followed by later eruption of more deeply sourced primitive magma. The composition of the mantle source appears homogeneous, being oxidized (fO_2 = +1.5 to +2 FMQ), with an apparent contribution from pyroxenite (X_{px} = 0.31 ±0.12) and with radiogenic $^{187}Os/^{188}Os$ (~0.145) consistent with a recycled HIMU-type oceanic lithosphere component. Combined with seismic data, lava samples provide a high-resolution record of eruption progression. Magma was emplaced at upper-lithospheric depths (8 to 45 km) at least four and possible ten years prior to eruption. Early erupted tephrites were sourced from upper portions of the magma storage system, with mixing between less differentiated basanitic magmas from deeper magma source regions beneath La Palma. This magmatic progression is like that inferred from the 1949 and 1971 Cumbre Vieja eruptions. Precursor events to the 2021 La Palma eruption involved early ground deformation, seismicity, underplating and magma fractionation at depth, followed by eruption and eventual exhaustion of stored magma batches at depth. Ocean islands with limited basaltic magma supply can evolve to more differentiated compositions during magma residence in the underplating and accumulation zone akin to large silicic systems where initial magma emplacement is usually followed by storage and differentiation via fractionation and assimilation with subsequent remobilization events.

CRediT authorship contribution statement

James Day: Conceptualization, Methodology, Resources, Writing – Original draft preparation, Sample collection, Funding Acquisition. **Valentin Troll:** Resources, Sample collection, Writing – Review & Editing. **Meritxell Aulinas:** Methodology, Resources, Logistics, Sample collection, Writing – Review & Editing. **Frances Deegan:** Methodology, Writing – Review & Editing. **Harri Geiger:** Sample collection, Writing – Review & Editing. **Juan Carlos Carracedo:** Sample collection, Logistics, Writing – Review & Editing. **Guillem Gisbert Pinto:** Sample collection, Logistics, Writing – Review & Editing. **Francisco Perez-Torrado:** Sample collection, Logistics, Writing – Review & Editing.

Declaration of competing interest

The authors declare that they have no known competing financial interests or personal relationships that could have appeared to influence the work reported in this paper.

Data availability

All new data associated with the manuscript are presented in the associated tables or supplementary tables.

Acknowledgements

The authors are grateful to PEVOLCA for enabling access to the Exclusion Zone of La Palma during the 2021 eruption for sample collection. We also thank S. Kelly (Scripps Institution of Oceanography) for help with sample preparation of the late lavas, A. Karlsson for SEM support (Swedish Museum of Natural History), H. Müller-Sigmund for EPMA support and G. Mette and M. Schrage for expedited sample preparation (University of Freiburg). Helpful comments and suggestions by C. Chauvel and an anonymous reviewer are gratefully acknowledged. Financial support came from: NSF EAR 1918322 (JMDD); the LAJIAL (PGC2018-101027-B-I00, MCIU/AEI/FEDER, EU) and MESVOL (SD RD 1078/2021 LA PALMA) research projects (FJPT and MA); the Swedish Research Council (Vetenskapsrådet grants 2018-04933 to FMD and 2020-03789 to VRT); the Section for Natural Resources and Sustainable Development at Uppsala University (FMD and VRT); and Friedrich-Rinne-Stiftung at the University of Freiburg (HG).

Appendix A. Supplementary material

Supplementary material related to this article can be found online at https://doi.org/10.1016/j.epsl.2022.117793.

References

Albert, H., Costa, F., Marti, J., 2015. Timing of magmatic processes and unrest associated with mafic historical monogenetic eruptions in Tenerife Island. J. Petrol. 56, 1945–1966.

Bachmann, O., Huber, C., 2016. Silicic magma reservoirs in the Earth's crust. Am. Mineral. 101, 2377–2404.

Barker, A.K., Troll, V.R., Carracedo, J.C., Nicholls, P.A., 2015. The magma plumbing system for the 1971 Teneguía eruption on La Palma, Canary Islands. Contrib. Mineral. Petrol. 170, 1–21.

Bindeman, I.N., Deegan, F.M., Troll, V.R., Thordarson, T., Hoskuldsson, A., Moreland, W.M., Zorn, E.U., Shevshenko, A.V., Walter, T.R., 2022. Diverse mantle components with invariant oxygen isotopes in the 2021 Fagradalsfjall eruption, Iceland. Nat. Commun. 13, 3737. https://doi.org/10.1038/s41467-022-31348-7.

Brounce, M.N., Stolper, E., Eiler, J., 2017. Redox variations in Mauna Kea lavas, the oxygen fugacity of the Hawaiian plume, and the role of volcanic gases in Earth's oxygenation. Proc. Natl. Acad. Sci. 114, 8997–9002.

Cashman, K.V., Sparks, R.S.J., Blundy, J.D., 2017. Vertically extensive and unstable magmatic systems: a unified view of igneous processes. Science 355, eaag3055.

Carracedo, J.C., Rodríguez Badiola, E., Soler, V., 1992. The 1730-1736 eruption of Lanzarote: an unusually long, high magnitude fissural basaltic eruption in the recent volcanism of the Canary Islands. J. Volcanol. Geotherm. Res. 53, 239–250.

Carracedo, J.C., Day, S., Guillou, H., Rodriguez-Badiola, E., Canas, J.A., Perez-Torrado, F.J., 1998. Hotspot volcanism close to a passive continental margin: the Canary Islands. Geol. Mag. 5, 591–604.

Carracedo, J.C., Rodriguez-Badiola, E., Guillou, H., Nuez Pestana, J.D.L., Pérez Torrado, F.J., 2001. Geology and volcanology of La Palma and El Hierro, western Canaries. Estud. Geol. 57, 175–273.

Carracedo, J.C., Torrado, F.P., González, A.R., Soler, V., Turiel, J.L.F., Troll, V.R., Wiesmaier, S., 2012. The 2011 submarine volcanic eruption in El Hierro (Canary Islands). Geol. Today, 53–58.

Carracedo, J.C., Troll, V.R., Zaczek, K., Rodríguez-González, A., Soler, V., Deegan, F.M., 2015. The 2011–2012 submarine eruption off El Hierro, Canary Islands: new lessons in oceanic island growth and volcanic crisis management. Earth-Sci. Rev. 150, 168–200.

Carracedo, J.C., Troll, V.R., 2016. The Geology of the Canary Islands. Elsevier. 621 pp.

Carracedo, J.C., Troll, V.R., Day, J.M.D., Geiger, H., Aulinas, M., Soler, V., Deegan, F., Pérez-Torrado, F.J., Gisbert, G., Gazel, E., Rodríguez-González, A., Albert, H., 2022. The 2021 eruption of the Cumbre Vieja Volcanic Ridge on La Palma, Canary Islands. Geol. Today 38, 94–107.

Cooper, K.M., Kent, A.J., 2014. Rapid remobilization of magmatic crystals kept in cold storage. Nature 506, 480–483.

Copernicus, 2022. European Union Earth observer program. https://www.copernicus.eu/en/news/news/observer-copernicus-eyes-la-palma-eruption.

Day, J.M.D., 2013. Hotspot volcanism and highly siderophile elements. Chem. Geol. 341, 50–74.

Day, J.M.D., Pearson, D.G., Macpherson, C.G., Lowry, D., Carracedo, J.-C., 2009. Pyroxenite-rich mantle formed by recycled oceanic lithosphere: oxygen-osmium isotope evidence from Canary Island lavas. Geology 37, 555–558.

Day, J.M.D., Pearson, D.G., Macpherson, C.G., Lowry, D., Carracedo, J.-C., 2010. Evidence for distinct proportions of subducted oceanic crust and lithosphere in HIMU-type mantle beneath El Hierro and La Palma, Canary Islands. Geochim. Cosmochim. Acta 74, 6565–6589.

Day, J.M.D., Walker, R.J., Warren, J.M., 2017. ^{186}Os-^{187}Os and highly siderophile element abundance systematics of the mantle revealed by abyssal peridotites and Os-rich alloys. Geochim. Cosmochim. Acta 200, 232–254.

Day, J.M.D., Maria-Benavides, J., McCubbin, F.M., Zeigler, R.A., 2018. The potential for metal contamination during Apollo lunar sample curation. Meteorit. Planet. Sci. 53, 1283–1291.

Fernández, J., Escayo, J., Hu, Z., Camacho, A.G., Samsonov, S.V., Prieto, J.F., Tiampo, K.F., Palano, M., Mallorquí, J.J., Ancochea, E., 2021. Detection of volcanic unrest onset in La Palma, Canary Islands, evolution and implications. Sci. Rep. 11, 1–15.

Galipp, K., Klügel, A., Hansteen, T.H., 2006. Changing depths of magma fractionation and stagnation during the evolution of an oceanic island volcano: La Palma (Canary Islands). J. Volcanol. Geotherm. Res. 155, 285–306.

Gleeson, M.L., Gibson, S.A., 2019. Crustal controls on apparent mantle pyroxenite signals in ocean-island basalts. Geology 47 (4), 321–324.

Global Volcanism Program, 2021. Report on La Palma (Spain). In: Sennert, S.K. (Ed.), Weekly Volcanic Activity Report. 24 November-30 November 2021. Smithsonian Institution and US Geological Survey.

González, P.J., 2022. Volcano-tectonic control of Cumbre Vieja. Science 375, 1348–1349.

Gurenko, A.A., Hoernle, K.A., Hauff, F., Schmincke, H.-U., Han, D., Miura, Y.N., Kaneoka, I., 2006. Major, trace element and Nd-Sr-Pb-O-He-Ar isotope signatures of shield stage lavas from the central and western Canary Islands: insights into mantle and crustal processes. Chem. Geol. 233, 75–112.

Gurenko, A.A., Sobolev, A.V., Hoernle, K.A., Hauff, F., Schmincke, H.-U., 2009. Enriched, HIMU-type peridotite and depleted recycled pyroxenite in the Canary plume: a mixed-up mantle. Earth Planet. Sci. Lett. 277, 514–524.

Hansteen, T.H., Troll, V.R., 2003. Oxygen isotope composition of xenoliths from the oceanic crust and volcanic edifice beneath Gran Canaria (Canary Islands): consequences for crustal contamination of ascending magmas. Chem. Geol. 193, 181–193.

Hart, S.R., Hauri, E.H., Oschmann, L.A., Whitehead, J.A., 1992. Mantle plumes and entrainment: isotopic evidence. Science 256, 517–520.

Herzberg, C., 2011. Identification of source lithology in the Hawaiian and Canary Islands: implications for origins. J. Petrol. 52, 113–146.

Hoernle, K.A.J., 1998. Geochemistry of Jurassic oceanic crust beneath Gran Canaria (Canary Islands): implications for crustal recycling and assimilation. J. Petrol. 39, 859–880.

Hoernle, K., Schmincke, H.-U., 1993. The role of partial melting in the 15-Ma geochemical evolution of Gran Canaria: a blob model for the Canary hotspot. J. Petrol. 34, 599–626.

Hoernle, K.A., Zhang, Y.-S., Graham, D.W., 1995. Seismic and geochemical evidence for large-scale mantle upwelling beneath the eastern Atlantic and western and central Europe. Nature 374, 34–39.

Hofmann, A.W., 1997. Mantle geochemistry: the message from oceanic volcanism. Nature 385, 219–229.

IGN, 2022. Catálogo de terremotos. Instituto Geográfico Nacional. https://www.ign.es/web/ign/portal/vlc-area-volcanologia.

Klügel, A., Hoernle, K.A., Schmincke, H.U., White, J.D., 2000. The chemically zoned 1949 eruption on La Palma (Canary Islands): petrologic evolution and magma supply dynamics of a rift zone eruption. J. Geophys. Res., Solid Earth 105 (B3), 5997–6016.

Klügel, A., Hansteen, T.H., Galipp, K., 2005. Magma storage and underplating beneath Cumbre Vieja volcano, la Palma (Canary Islands). Earth Planet. Sci. Lett. 236, 211–226.

Klügel, A., Galipp, K., Hoernle, K., Hauff, F., Groom, S., 2017. Geochemical and volcanological evolution of La Palma, Canary Islands. J. Petrol. 58, 1227–1248.

Klügel, A., Albers, E., Hansteen, T.H., 2022. Mantle and crustal xenoliths in a tephriphonolite from La Palma (Canary Islands): implications for phonolite formation at oceanic island volcanoes. Front. Earth Sci. 10. https://doi.org/10.3389/feart.2022.761902.

Koushelar, M., Widom, E., Kuentz, D., 2021. Osmium isotope geochemistry of steel plant emissions using tree bark biomonitoring. Environ. Pollut. 272, 115976.

Longpré, M.-A., 2021. Reactivation of the Cumbre Vieja Volcano. Science 374, 1197–1198.

Longpré, M.-A., Klügel, A., Diehl, A., Stix, J., 2014. Mixing in mantle magma reservoirs prior to and during the 2011-2012 eruption at El Hierro, Canary Islands. Geology 42, 315–318.

Lynn, K.J., Shea, T., Garcia, M.O., 2017. Nickel variability in Hawaiian olivine: evaluating the relative contributions from mantle and crustal processes. Am. Mineral. 102, 507–518.

Marcantonio, F., Zindler, A., Elliott, T., Staudigel, H., 1995. Os isotope systematics of La Palma, Canary Islands: evidence for recycled crust in the mantle source of HIMU ocean islands. Earth Planet. Sci. Lett. 133, 397–410.

Martí, J., Castro, A., Rodríguez, C., Costa, F., Carrasquilla, S., Pedreira, R., Bolos, X., 2013. Correlation of magma evolution and geophysical monitoring during the 2011-2012 El Hierro (Canary Islands) submarine eruption. J. Petrol. 54, 1349–1373.

McDonough, W.F., Sun, S.-S., 1995. The composition of the Earth. Chem. Geol. 120, 223–253.
McKenzie, D., O'Nions, R.K., 1991. Partial melt distributions from inversion of rare Earth element concentrations. J. Petrol. 32, 1021–1091.
Meletlidis, S., Di Roberto, A., Pompilio, M., Bertagnini, A., Iribarren, I., Felpeto, A., Torres, P.A., D'Oriano, C., 2012. Xenopumices from the 2011–2012 submarine eruption of El Hierro (Canary Islands, Spain): constraints on the plumbing system and magma ascent. Geophys. Res. Lett. 39 (17).
Meletlidis, S., Di Roberto, A., Cerdeña, I.D., Pompilio, M., Bertagnini, A., Benito-Saz, M.A., Aparicio, S.S.M., 2015. New insight into the 2011-2012 unrest and eruption of El Hierro Island (Canary Islands) based on integrated geophysical, geodetical and petrological data. Ann. Geophys. 58, S0546.
Moussallam, Y., et al., 2019. Mantle plumes are oxidized. Earth Planet. Sci. Lett. 527, 115798.
Nicklas, R.W., Puchtel, I.S., Ash, R.D., Piccoli, P.M., Hanski, E., Nisbet, E.G., Waterton, P.M., Pearson, D.G., Anbar, A.D., 2019. Secular mantle oxidation across the Archean-Proterozoic boundary: evidence from V partitioning in komatiites and picrites. Geochim. Cosmochim. Acta 250, 49–75.
Nicklas, R.W., Hahn, R.K.M., Day, J.M.D., 2022a. Oxidation of La Réunion lavas with MORB-like fO_2 by assimilation. Geochem. Perspect. Lett. 20, 32–36.
Nicklas, R.W., Hahn, R.K.M., Willhite, L.N., Jackson, M.G., Zanon, V., Arevalo, R., Day, J.M.D., 2022b. Oxidized mantle sources of HIMU and EM-type ocean island basalts. Chem. Geol. 602, 120901.
Nisbet, E.G., Cheadle, M.J., Arndt, N.T., Bickle, M.J., 1993. Constraining the potential temperature of the Archean mantle: a review of the evidence from komatiites. Lithos 30, 291–307.
Pankhurst, M.J., Scarrow, J.H., Barbee, O.A., Hickey, J., Coldwell, B.C., Rollinson, Rodriguez-Losada, J.A.R., Martín-Lorenzo, A., Rodríguez, F., Hernández, W., Hernández, P.A., Pérez, N.M., 2021. Petrology of the opening eruptive phase of the 2021 Cumbre Vieja eruption, La Palma, Canary Islands. Volcanica 5, 1–10.
PEVOLCA, 2021. Plan Especial de Protección Civil y Atención de Emergencias por riesgo volcánico en la Comunidad Autónoma de Canarias. https://info.igme.es/eventos/Erupcion-volcanica-la-palma/pevolca.
Reisberg, L., Zindler, A., Marcantonio, F., White, W., Wyman, D., Weaver, B., 1993. Os isotope systematics in ocean island basalts. Earth Planet. Sci. Lett. 120, 149–167.
Sobolev, A.V., et al., 2007. The amount of recycled crust in sources of mantle-derived melts. Science 316, 412–417.
Taracsák, Z., Longpré, M.A., Tartèse, R., Burgess, R., Edmonds, M., Hartley, M.E., 2022. Highly oxidising conditions in volatile-rich El Hierro magmas: implications for ocean island magmatism. J. Petrol. 63, egac011.
Torres-González, P.A., Luengo-Oroz, N., Lamolda, H., D'Alessandro, W., Albert, H., Iribarren, I., Moure-García, D., Soler, V., 2020. Unrest signals after 46 years of quiescence at cumbre vieja, la palma, Canary Islands. J. Volcanol. Geotherm. Res. 392.
Turner, S., Hoernle, K., Hauff, F., Johansen, T.S., Klügel, A., Kokfelt, T., Lundstrom, C., 2015. 238 U–230 Th–226 Ra disequilibria constraints on the magmatic evolution of the Cumbre Vieja volcanics on La Palma, Canary Islands. J. Petrol. 56, 1999–2024.
Troll, V.R., Klügel, A., Longpré, M.A., Burchardt, S., Deegan, F.M., Carracedo, J.C., Wiesmaier, S., Kueppers, U., Dahrén, B., Blythe, L.S., Hansteen, T.H., 2012. Floating stones off El Hierro, Canary Islands: xenoliths of pre-island sedimentary origin in the early products of the October 2011 eruption. Solid Earth 3, 97–110.
Vlastélic, I., Deniel, C., Bosq, C., Télouk, P., Boivin, P., Bachèlery, P., Famin, V., Staudacher, T., 2009. Pb isotope geochemistry of Piton de la Fournaise historical lavas. J. Volcanol. Geotherm. Res. 184, 63–78.
Wang, J., Xiong, X., Takahashi, E., Zhang, L., Li, L., Liu, X., 2019. Oxidation state of arc mantle revealed by partitioning of V, Sc and Ti between mantle minerals and basaltic melts. J. Geophys. Res., Solid Earth 124, 4617–4638.
Widom, E., Hoernle, K.A., Shirey, S.B., Schmincke, H.-U., 1999. Os isotope systematics in the Canary Islands and Madeira: lithospheric contamination and mantle plume signatures. J. Petrol. 40, 279–296.
Winterbourne, J., Crosby, A., White, N., 2009. Depth, age and dynamic topography of oceanic lithosphere beneath heavily sedimented Atlantic margins. Earth Planet. Sci. Lett. 287, 137–151.
Zanon, V., Cyrzan, K., D'Auria, L., Pankhurst, M., Rodríguez, F., Coldwell, B., Martín-Lorenzo, A., 2022. The magma ascent path during the 2021 eruption of Cumbre Vieja (La Palma Island, Canary archipelago) highlighted by fluid inclusions and seismicity. EGU General Assembly 2022. https://doi.org/10.5194/egusphere-egu22-10203.
Zaczek, K., Troll, V.R., Cachao, M., Ferreira, J., Deegan, F.M., Carracedo, J.C., Soler, V., Meade, F.C., Burchardt, S., 2015. Nannofossils in 2011 El Hierro eruptive products reinstate plume model for Canary Islands. Sci. Rep. 5, 1–5.
Zindler, A., Hart, S.R., 1986. Chemical geodynamics. Annu. Rev. Earth Planet. Sci. 14, 493–571.